M = equilibrium constant
m_0 = equilibrium constant parameter, dimensionless (2)
n = number of cycles of pump operation
p_1, p_2 = defined by Equations (6) and (10)
Q = reservoir displacement rate, cu.cm./sec.
q_1, q_2 = defined by Equations (6) and (10)
v_0 = interstitial velocity, m./sec.
V_T = top dead reservoir volume, cu.cm.
V_B = bottom dead reservoir volume, cu.cm.
y = concentration of solute in the liquid phase, kg.-mole/cu.cm.
$< >$ = average value

Greek Letters

χ = concentration of solute in the solid phase, kg.-mole/Kg.
ϕ = product volumetric flow rate/reservoir displacement rate, dimensionless
$\frac{\pi}{\omega}$ = duration of half cycle, sec.

Subscripts

0 = initial condition
1 = upflow
2 = downflow
BP = bottom product
TP = top product
B = stream from or to bottom of the column
T = stream from or to top of the column

LITERATURE CITED

1. Wilhelm, R. H., and N. H. Sweed, *Science,* **159,** 522 (1968).
2. Pigford, R. L., B. Baker, and D. E. Blum, *Ind. Eng. Chem., Fundamentals,* **8,** 144 (1969).
3. Chen, H. T., and F. B. Hill, *Separ. Sci.,* **6,** 411 (1971).
4. Chen, H. T., and F. B. Hill, unpublished work (1970).
5. Sweed, N. H., Ph.D. dissertation, Princeton Univ., Princeton, N. J. (1969).
6. Wilhelm, R. H., A. W. Rice, R. W. Rolke, and N. H. Sweed, *Ind. Eng. Chem. Fundamentals,* **7,** 337 (1968).

Manuscript received July 27, 1971; revision received September 3, 1971; paper accepted October 26, 1971.

Forced Convection Heat Transfer Correlations for Flow in Pipes, Past Flat Plates, Single Cylinders, Single Spheres, and for Flow in Packed Beds and Tube Bundles

STEPHEN WHITAKER

Department of Chemical Engineering
University of California, Davis, Calif. 95616

Previously obtained experimental heat transfer data have been collected and are illustrated along with minor variations of the standard correlations. Analysis of data for heat transfer in randomly packed beds and compact (void fraction less than 0.65) staggered tube bundles indicates that the Nusselt number for a wide range of packing materials and tube arrangements is given by

$$N_{Nu} = (0.5\, N_{Re}^{1/2} + 0.2\, N_{Re}^{2/3})\, N_{Pr}^{1/3}\, (\mu_b/\mu_0)^{0.14}$$

provided $N_{Re} \geqq 50$. The correlations presented in this paper are not necessarily the most accurate available; however, they have wide application, are easy to use, and are quite satisfactory for most design calculations.

For the past forty years there has been a steady effort to improve our knowledge of forced convection heat transfer rates for a variety of important process configurations. It is of value to periodically review the experimental data and construct new correlations on the basis of new data and theoretical advances. McAdams (23) contributed much along these lines in 1954; however, enough new data have been obtained so that these correlations deserve a second look.

All the experimental data that we wish to consider in this paper can be satisfactorily described in terms of the following equations:
equations of motion

$$\rho\left(\frac{\partial \mathbf{v}}{\partial t} + \mathbf{v}\cdot\nabla\mathbf{v}\right) = -\nabla p + \rho\mathbf{g} + \nabla\cdot\boldsymbol{\tau} \qquad (1)$$

constitutive equation for a Newtonian fluid

$$\boldsymbol{\tau} = \mu\,(\nabla\mathbf{v} + \nabla\mathbf{v}^{+}) \qquad (2)$$

continuity equation

$$\nabla\cdot\mathbf{v} = 0 \qquad (3)$$

thermal energy equation

$$\rho c_p \left(\frac{\partial T}{\partial t} + (\mathbf{v} \cdot \underset{\sim}{\nabla} T) \right) = k \nabla^2 T \tag{4}$$

The form of these equations indicates that we are considering the density and thermal conductivity ρ and k to be constant. In addition we will take c_p to be a constant while allowing the viscosity μ to be a function of temperature. Substitution of Equation (2) into Equation (1) leads to

$$\rho \left(\frac{\partial \mathbf{v}}{\partial t} + \mathbf{v} \cdot \underset{\sim}{\nabla} \mathbf{v} \right) = - \underset{\sim}{\nabla} p + \rho \mathbf{g} + \mu \nabla^2 \mathbf{v} + (\underset{\sim}{\nabla} \mu) \cdot (\underset{\sim}{\nabla} \mathbf{v} + \underset{\sim}{\nabla} \mathbf{v}^+) \tag{5}$$

Since we are taking the viscosity to be a function of temperature alone, we can write

$$\underset{\sim}{\nabla} \mu = \left(\frac{\partial \mu}{\partial T} \right) (\underset{\sim}{\nabla} T) \tag{6}$$

In addition we can write a Taylor series expansion for μ about the reference temperature T^*.

$$\mu(T) = \mu^* + \left(\frac{\partial \mu}{\partial T} \right)^* (T - T^*) + \frac{1}{2!} \left(\frac{\partial^2 \mu}{\partial T^2} \right)^* (T - T^*)^2 + \ldots \tag{7}$$

Here the asterisk superscript indicates that the function is evaluated at the reference temperature T^*. We can now express Equation (5) as

$$\rho \left(\frac{\partial \mathbf{v}}{\partial t} + \mathbf{v} \underset{\sim}{\nabla} \cdot \mathbf{v} \right) = - \underset{\sim}{\nabla} p + \rho \mathbf{g} + \mu^* \left[1 + \frac{1}{\mu^*} \left(\frac{\partial \mu}{\partial T} \right)^* (T - T^*) \right] \nabla^2 \mathbf{v} + \left(\frac{\partial \mu}{\partial T} \right)^* (\underset{\sim}{\nabla} T) \cdot (\underset{\sim}{\nabla} \mathbf{v} + \underset{\sim}{\nabla} \mathbf{v}^+) \tag{8}$$

The higher order terms in the Taylor series expansion have been dropped, thus we are restricting our analysis to the first order effect of temperature on the viscosity. Choosing the characteristic length as L^* and the characteristic velocity as u^* we can put Equations (3), (4), and (8) in dimensionless form to obtain

$$\left(\frac{\partial \mathbf{U}}{\partial \theta} \right) + \mathbf{U} \cdot \underset{\sim}{\nabla} \mathbf{U} = - \underset{\sim}{\nabla} P + \frac{1}{N_{Re}} [1 + \Lambda \Theta] \nabla^2 \mathbf{U} + \frac{1}{N_{Re}} [\Lambda (\underset{\sim}{\nabla} \Theta) \cdot (\underset{\sim}{\nabla} \mathbf{U} + \underset{\sim}{\nabla} \mathbf{U}^+)] \tag{9}$$

$$\underset{\sim}{\nabla} \cdot \mathbf{U} = 0 \tag{10}$$

$$\frac{\partial \Theta}{\partial \theta} + \mathbf{U} \cdot \underset{\sim}{\nabla} \Theta = \frac{1}{N_{Re} N_{Pr}} \nabla^2 \Theta \tag{11}$$

Here we have used the following definitions

$\mathbf{U} = \mathbf{v}/u^*$, dimensionless velocity vector

$\underset{\sim}{\nabla} = L^* \nabla$, dimensionless "del" operator

$P = \frac{p - p^*}{\rho u^{*2}} + \frac{\phi}{u^{*2}}$, dimensionless pressure which includes the body force

$N_{Re} = \rho u^* L^*/\mu$, Reynolds number

$\Lambda = \frac{1}{\mu} \left(\frac{\partial \mu}{\partial \Theta} \right)$, dimensionless viscosity parameter

$\theta = t u^*/L^*$, dimensionless time

$\Theta = (T - T^*)/(T_0 - T^*)$, dimensionless temperature. T^* and T_0 are often chosen so that $0 \leq \Theta \leq 1$

$N_{Pr} = c_p \mu/k$

where it is understood that all physical properties are evaluated at the reference temperature. At this point we can specify the functional dependence of the dimensionless temperature as

$$\Theta = F \{ \underbrace{(\theta, X, Y, Z)}_{\text{independent variables}}, \underbrace{(N_{Re}, N_{Pr}, \Lambda)}_{\text{parameters appearing in the differential equations}} \underbrace{(N_{BC})}_{\text{parameters appearing in the boundary conditions}} \} \tag{12}$$

We will not discuss the parameters which appear in the dimensionless form of the boundary conditions; however, we will carry the term N_{BC} as a reminder that one must always carefully consider the boundary condition.

CHOICE OF REFERENCE TEMPERATURE

In the analysis of heat transfer processes the bulk or "cup mixing" temperature is the most convenient temperature to use in the macroscopic balances. This temperature will be denoted by T_b and is defined by

$$T_b = \frac{\int_A T \, \mathbf{v} \cdot \mathbf{n} dA}{\int_A \mathbf{v} \cdot \mathbf{n} dA} \tag{13}$$

For the case of flow past bodies immersed in an infinite fluid the bulk temperature becomes the free stream temperature

$$T_b = T_\infty, \quad \text{for bodies immersed in an infinite fluid} \tag{14}$$

In many of the early heat transfer studies the film temperature T_f was taken as the reference temperature. It is defined as

$$T_f = \frac{1}{2} (T_b + T_0) \tag{15}$$

where T_0 is the surface or wall temperature. We should be very careful to understand at this point that Θ depends on N_{Re}, N_{Pr}, and Λ *regardless* of the choice of the reference temperature. It is true that one or the other of these temperatures may represent a "better" choice of a reference temperature, thus minimizing the functional dependence of Θ on Λ. Indeed, in the early work on forced convection heat transfer it was assumed that use of the film temperature as a reference temperature would essentially eliminate any dependence on Λ; however, a number of recent studies using highly viscous oils indicate that use of the bulk temperature and a parameter comparable to Λ is the preferable method of correlating the data.

In order to illustrate how one makes use of the parameter Λ, let us consider the problem of heat transfer in a pipe for the following conditions:

1. wall temperature is constant at T_0
2. bulk temperature at the entrance is T_{b1}
3. bulk temperature at the exit is T_{b2}

We choose the reference temperature to be the average bulk temperature

$$T^* = \frac{1}{2}(T_{b1} + T_{b2}) \tag{16}$$

and note that an order of magnitude estimate of Λ is given by

$$\Lambda = \frac{1}{\mu}\left(\frac{\partial \mu}{\partial \Theta}\right) \approx \frac{1}{\mu^*}\left[\frac{\mu^* - \mu_0}{0 - 1}\right] = \left[\frac{\mu_0}{\mu^*} - 1\right] \tag{17}$$

In arriving at this result we have used the fact that Θ is given by

$$\Theta = \frac{T - T^*}{T_0 - T^*} \tag{18}$$

and thus varies from 1 at the wall where $T = T_0$ to approximately zero at the center of the pipe where $T \approx \frac{1}{2}(T_{b1} + T_{b2})$. We now see that the effect of variable viscosity can be correlated by the ratio* of viscosities μ_b/μ_0, but we must remember that this result is based on retaining only the first term in a Taylor series expansion of μ, and the order of magnitude estimate given by Equation (17). For steady state processes we can now express the functional dependence of the Nusselt number as

$$N_{Nu} = hL^*/k$$
$$= F(N_{Re}, N_{Pr}, \mu_b/\mu_0, N_{BC}) \tag{19}$$

Discussion

Having decided upon the functional dependence of the Nusselt number for the case where only the viscosity is allowed to vary with temperature, we are in a position to consider the experimental data.

LAMINAR FLOW IN A PIPE

When the restriction $N_{Re}N_{Pr} > 100$ is satisfied (*35*) the heat transfer process is adequately described by the Graetz solution (*18*). An empirical modification of the Graetz solution has been given by Sieder and Tate (*37*) for the case where the viscosity is a function of temperature.

$$N_{Nu} = 1.86\, N_{Re}^{1/3}\, N_{Pr}^{1/3}\, (L/D)^{-1/3}\, (\mu_b/\mu_0)^{0.14} \tag{20}$$

In this expression the physical properties of the fluid are evaluated at the reference temperature, that is, the mean or average bulk temperature. The ratio (μ_b/μ_0) represents the ratio of the viscosity evaluated at the mean bulk temperature to the viscosity evaluated at the mean wall temperature. The solution to the Graetz problem indicates that for very long tubes

$$N_{Nu} = 3.66, \quad L/D \to \infty \tag{21}$$

When the viscosity is a function of temperature this result can be approached asymptotically from either above or

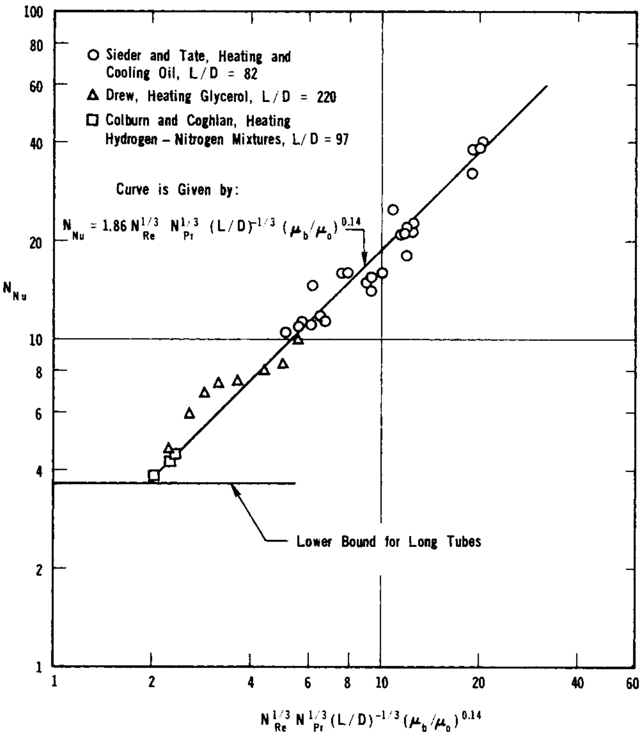

Fig. 1. Heat transfer to fluids in laminar flow in tubes.

* Here μ_b represents the viscosity evaluated at the average bulk temperature, thus $\mu_b = \mu^*$.

TABLE 1.

Process	Definition of Reynolds number	Definition of Nusselt number	Definition of h	Reference temp., T^*	Range of Reynolds number	Range of Prandtl number	Range of (μ_b/μ_0)
Laminar flow in a pipe	$<v_z>D/\nu_b$	hD/k_b	$\dot{Q}/\pi DL\Delta T_{ln}$	$\frac{1}{2}(T_{b1} + T_{b2})$	13-2,030	0.48-16,700	0.0044-9.75
Turbulent flow in a pipe	$<v_z>D/\nu_b$	hD/k_b	$\dot{Q}/\pi DL\Delta T_{ln}$	$\frac{1}{2}(T_{b1} + T_{b2})$	$2.3 \times 10^3 - 1 \times 10^5$	0.48-592	0.44-2.5
Flow past a flat plate	$u_\infty L/\nu_\infty$	hL/k_∞	$\dot{Q}/2wL\,(T_0 - T_\infty)$	T_∞	$1 \times 10^5 - 5.5 \times 10^6$	0.70-380	0.26-3.5
Flow past a single sphere	$u_\infty D/\nu_\infty$	hD/k_∞	$\dot{Q}/4\pi D^2\,(T_0 - T_\infty)$	T_∞	$3.5 - 7.6 \times 10^4$	0.71-380	1.0-3.2
Flow past a single cylinder	$u_\infty D/\nu_\infty$	hD/k_∞	$\dot{Q}/\pi DL\,(T_0 - T_\infty)$	T_∞	$1.0 - 1 \times 10^5$	0.67-300	0.25-5.2
Flow in packed beds	$D_pG/\mu_f\,(1 - \epsilon)$	$\left(\frac{hD_p}{k_f}\right)\frac{\epsilon}{1-\epsilon}$	$\dot{Q}/a_v V\,\Delta T_{ln}$	$\frac{1}{2}(T_{f1} + T_{f2})$	$22\text{-}8 \times 10^3$	0.7	1
Flow in staggered tube bundles	$D_pG/\mu_b\,(1 - \epsilon)$*	$\left(\frac{hD_p}{k_b}\right)\frac{\epsilon}{1-\epsilon}$	$\dot{Q}/a_v V\,\Delta T_{ln}$	$\frac{1}{2}(T_{b1} + T_{b2})$	$1.0\text{-}10^5$	0.7-760	0.18-4.3

* D_p for tube bundles is given by $D_p = \dfrac{6V_p}{A_p} = \dfrac{3}{2}D$.

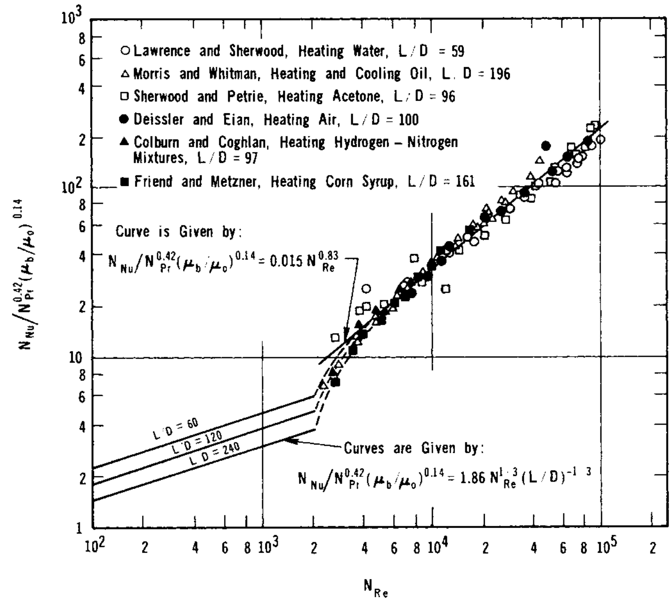

Fig. 2. Heat transfer to fluids in turbulent flow in tubes.

below (*47*). In Figure 1 we have compared Equation (20) with the experimental data of three investigations (*7, 15, 37*). The agreement obtained by three different investigators for a fairly wide range of the dimensionless parameters is certainly very pleasing and indicates that the Sieder-Tate correlation is quite satisfactory. This particular process has been analyzed in some detail by a number of investigators (*4, 5, 25*) and without question there are better expressions available for the Nusselt number; however, Equation (20) and other correlations presented in this paper are given with the idea that in the course of the design, construction, and operation of most heat transfer equipment there will be considerable uncertainty and there is little need for using correlations which introduce far less uncertainty than that produced by the design, construction, and operation. The range of the dimensionless parameters for the data shown in Figure 1 and the definitions of N_{Re} and N_{Nu} are given in Table 1. In plotting the Nusselt number against $(N_{Re} N_{Pr}\ D/L)^{1/3}$ we may be guilty of what Colburn (*8*) referred to as plotting a function against itself, and there are many who would suggest at this point that the use of a *j*-factor or Stanton number would be more appropriate. A detailed discussion of this point is given in the appendix, and there it is shown that there is no preference for the *j*-factor or Stanton number over the Nusselt number. One must always be careful in viewing plots such as the one shown in Figure 1 to remember that the scale is logarithmic, and experimental error tends to be obscured. The error in the experimentally determined Nusselt numbers is on the order of $\pm$ 25%.

TURBULENT FLOW IN A PIPE

The experimental data of a number of investigators (*7, 10, 15, 22, 26, 28*) for turbulent pipe flow are shown in Figure 2. The Nusselt number is quite nicely correlated by the expression

$$N_{Nu} = 0.015\ N_{Re}^{0.83}\ N_{Pr}^{0.42}\ (\mu_b/\mu_0)^{0.14} \qquad (22)$$

The Prandtl number dependence is based on the work of Friend and Metzner (*15*), the functional dependence of (μ_b/μ_0) is from the work of Sieder and Tate (*37*), and the coefficient 0.015 and the Reynolds number dependence are in general agreement with a more thorough survey of the turbulent Graetz problem by Notter and Sleicher (*27*). The data of Friend and Metzner (*15*) for corn syrup, and the data of Deissler and Eian for air (*10*), represent the most recent and most accurate experimental values; however, one should note that the pioneering work of Morris and Whitman, performed prior to 1927, has rather nicely withstood the test of time. Once again one must remember that the logarithmic scale tends to hide the experimental error which is on the order of $\pm$ 15%. For a more accurate correlation the interested reader is referred to the recent work of Notter and Sleicher (*27*). The range of variables represented in Figure 2 and the definitions of N_{Re} and N_{Nu} are again listed in Table 1.

FLOW PAST A FLAT PLATE

For Prandtl numbers ranging from 0.6 to 10, a reasonable expression for the local Nusselt number in the laminar boundary layer (*34*) is

$$N_{Nu,x} = 0.332\ N_{Re,x}^{1/2}\ N_{Pr}^{1/3}, \quad \text{laminar boundary layer} \qquad (23)$$

On the basis of the experimental work of Zhukauskas and Ambrazyavichyus (*45*) we can modify Colburn's (*8*) empirical expression for the local Nusselt number in a turbulent boundary layer to obtain

$$N_{Nu,x} = 0.029\ N_{Re,x}^{0.8}\ N_{Pr}^{0.43}, \quad \text{turbulent boundary layer} \qquad (24)$$

If we assume that the transition takes place at a length Reynolds number of 2×10^5, and if we assume that Equation (23) is valid before the transition and Equation (24) is valid after the transition we can determine the average Nusselt number to be

$$N_{Nu} = 0.036\ (N_{Re,L}^{0.8}\ N_{Pr}^{0.43} - 17{,}400) + 297\ N_{Pr}^{1/3} \qquad (25)$$

For Prandtl numbers near unity we can write

$$297\ N_{Pr}^{1/3} \approx 297\ N_{Pr}^{0.43} \qquad (26)$$

and Equation (30) can be simplified to

$$N_{Nu} = 0.036\ N_{Pr}^{0.43}\ (N_{Re,L}^{0.8} - 9{,}200) \qquad (27)$$

The data of Zhukauskas and Ambrazyavichyus indicate that the dependence of the Nusselt number on the viscosity should be of the form $(\mu_x/\mu_0)^{1/4}$ thus Equation (27) can be expressed as

$$N_{Nu} = 0.036\ N_{Pr}^{0.43}\ (N_{Re,L}^{0.8} - 9{,}200)\ (\mu_x/\mu_0)^{1/4} \qquad (28)$$

If the Reynolds number is very large relative to the critical Reynolds number Equation (28) takes the simplified form

$$N_{Nu} = 0.036\ N_{Pr}^{0.43}\ N_{Re,L}^{0.8}\ (\mu_x/\mu_0)^{1/4} \qquad (29)$$

Both Equations (28) and (29) are compared with experimental data in Figure 3. Although a comparison is not shown, the data of Parmalee and Huebscher (*28*) and the data of Edwards and Furber (*12*) for negligible free stream turbulence are in excellent agreement with the average Nusselt number obtained from Equation (23) provided the Reynolds number is less than 2×10^5. For values of $N_{Re} > 2 \times 10^5$ the data of Parmalee and Huebscher show a sudden increase in N_{Nu} with the data being well represented by Equation (28). When great care is taken to eliminate free stream turbulence the transition is delayed and the Nusselt number is lower than that predicted by Equation (28). This is the case of the negligible free stream turbulence data of Edwards and Furber. When high intensity turbulence is generated in the free stream the transition to turbulence takes place at a lower Reynolds number and the Nusselt number is larger than that predicted by Equation (28). This is the case for the 5% free stream turbulence data of Edwards and Furber, which lie very close to the line of given by Equation (29). Although the level of turbulence was not specified by Zhukauskas and Ambrazyavichyus it is clear from their results that a high level of turbulence was present in the free stream. The effect of free stream turbulence illustrated in these heat transfer data is in good agreement with the experimental studies on laminar boundary layer stability performed by Schubauer and Skramstad (*36*). The functional dependence of the Nusselt number on the Prandtl number is essentially identical to that found for turbulent pipe flow; however, the dependence on the viscosity ratio (μ_b/μ_0) or (μ_x/μ_0) is considerably different. In considering this point one must remember that pinning down the best exponent for the viscosity ratio is indeed a very difficult experimental task, and one could easily look upon the difference between 0.14 and 0.25 as being due to experimental uncertainty. In addition we must keep in mind that the Nusselt number is influenced by the temperature dependence of the viscosity in some *complex* manner, thus, much of the experimental uncertainty could result from trying to force a *simple* functional relation to describe a *complex* phenomena. The range of variables for the data presented in Figure 3 are listed in Table 1.

FLOW PAST A SINGLE SPHERE

In treating flow past a single sphere we must make use of the fact that a steady state conduction solution exists (3) which yields

$$N_{Nu} = 2, \quad \text{steady state conduction solution} \qquad (30)$$

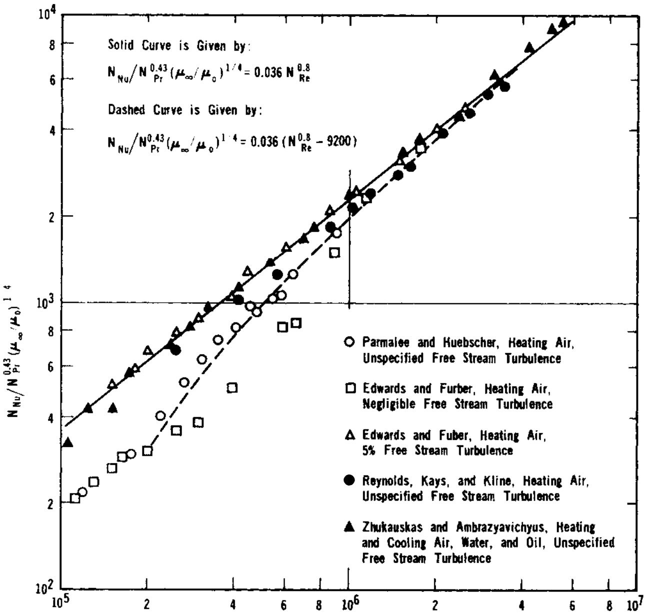

Fig. 3. Heat transfer to fluids flowing past a flat plate.

provided the sphere is immersed in an infinite media. In choosing a functional dependence on N_{Re}, N_{Pr} and (μ_b/μ_0) we begin with the form

$$(N_{Nu} - 2) = F(N_{Re}, N_{Pr}, \mu_b/\mu_0) \qquad (31)$$

subject to the restriction that $F(N_{Re}) \to 0$ as $N_{Re} \to 0$. In considering the functional dependence for the Reynolds number we refer to the work of Richardson (*33*) who recommended that the heat transfer from the sphere be considered as two parallel processes. In the laminar boundary layer region the contribution to the Nusselt number should be of the form $N_{Re}^{1/2} N_{Pr}^{1/3}$, while in the wake region Richardson argues that the contribution should be of the form $N_{Re}^{2/3} N_{Pr}^{1/3}$, so that Equation (31) could be expressed as

$$(N_{Nu} - 2) = (aN_{Re}^{1/2} + bN_{Re}^{2/3})\, N_{Pr}^{1/3}\, (\mu_b/\mu_0)^c \qquad (32)$$

On the basis of the work of Vliet and Leppert (*40*) and the supporting data of Kramers (*21*) the exponent on the Prandtl number is chosen to be 0.4 and the exponent on the viscosity ratio is taken to be 1/4. The constants a and b are chosen to obtain a good fit with the experimental data, and the final form of Equation (32) is

$$(N_{Nu} - 2) = (0.4\, N_{Re}^{1/2} + 0.06\, N_{Re}^{2/3}) N_{Pr}^{0.4}\, (\mu_b/\mu_0)^{1/4} \qquad (33)$$

This expression is rearranged slightly and compared with experimental data in Figure 4. The agreement is quite good, the scatter of the data around the correlation being ± 30% at the very worst. Once again the range of values of the parameters are listed in Table 1.

FLOW PAST A SINGLE CYLINDER

In developing a correlation for heat transfer from a single cylinder we note that no steady state conduction solutions exists, thus we require that

$$N_{Nu} \to 0 \quad \text{as} \quad N_{Re} \to 0$$

The success of the form used for correlating the sphere data motivates us to propose a correlation of the form

$$N_{Nu} = (0.4\, N_{Re}^{1/2} + 0.06\, N_{Re}^{2/3})\, N_{Pr}^{0.4}\, (\mu_b/\mu_0)^{1/4} \qquad (34)$$

The comparison of Equation (34) with the data of a number of investigators (*6, 9, 14, 19, 29, 31, 46*) is shown in Figure 5. The agreement is generally within ± 25% except in the region of low Reynolds numbers where the data of Hilpert and King are considerably higher than that predicted by Equation (34). More recent data obtained by Collis and Williams (*48*) for air are in reasonable agreement with the data of King and Hilpert. For Reynolds numbers in the range of 0.02 to 44 and small temperature difference Collis and Williams were able to correlate their data with the expression

$$N_{Nu} = 0.24 + 0.56\, N_{Re}^{0.45}, \quad \text{for air with negligible variation in the viscosity}$$

For this case Equation (34) reduces to

$$N_{Nu} = 0.35\, N_{Re}^{1/2} + 0.052\, N_{Re}^{2/3}$$
for air with negligible variation in the viscosity

Taking $N_{Re} = 1$ the Collis-Williams correlation predicts a value of 0.80 for the Nusselt number, while the correlation given in this paper yields a value of 0.40. One of the drawbacks to the Collis-Williams correlation is that it does not satisfy the theoretical restriction that $N_{Nu} \rightarrow 0$ as $N_{Re} \rightarrow 0$; nevertheless, it represents the results of some very careful experimental work and is in good agreement with the data of King and Hilpert. Clearly there is a need for more theoretical and experimental studies for Reynolds numbers less than 10.

It is convenient that we can correlate both cylinder and sphere data with essentially the same equation; however, one must keep in mind that the coefficients and powers on the Reynolds number are not sacrosanct. We are attempting to model the functional dependence of N_{Nu} on N_{Re} with a function of the form: $aN_{Re}{}^{b} + cN_{Re}{}^{d}$, and with four adjustable constants one could find other choices which might fit the data better than Equation (34). In any event there is some theoretical justification of the form of both Equations (33) and (34) and they do fit the data reasonably well. The range of variables illustrated in Figure 5 is listed in Table 1.

FLOW IN PACKED BEDS

In general the log-mean film heat transfer coefficient for a packed bed is defined as follows

$$\dot{Q} = h_{\ln}\, a_v V\, \Delta T_{\ln} \tag{35}$$

Here $\dot{Q}$ is the total rate of heat transfer from the packing to the fluid, $h_{\ln}$ is the film heat transfer coefficient defined by Equation (35), a_v is the packing surface area per unit volume, V is the total volume of the packed bed, and $\Delta T_{\ln}$ is the log-mean temperature difference.

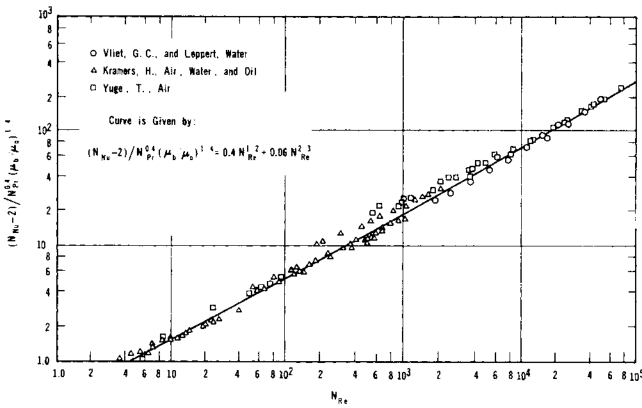

Fig. 4. Heat transfer to fluids flowing past a single sphere.

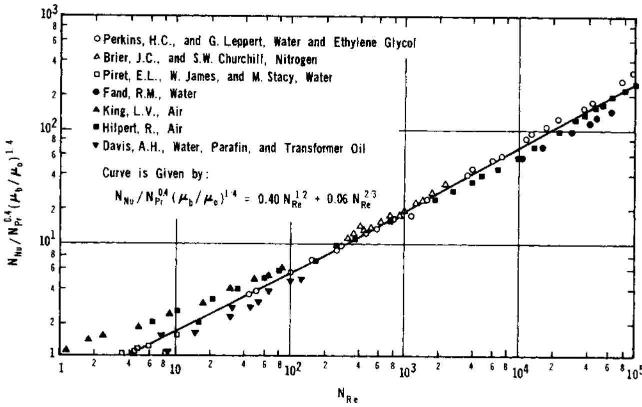

Fig. 5. Heat transfer to fluids flowing normal to a single cylinder.

The surface area per unit volume a_v can be related to the void fraction ϵ which is defined as

$$\epsilon = \frac{\text{void volume in the bed}}{\text{total volume of the bed}} = \frac{V_{\text{void}}}{V} \tag{36}$$

Consider a bed of volume V packed with N particles which have a volume V_p and a surface area A_p. If the void fraction in the bed is ϵ, the volume occupied by the particles is $V(1-\epsilon)$, thus we can write

$$V_p N = V(1-\epsilon) \tag{37}$$

This result can be rearranged to give the number of particles per unit volume as

$$N/V = (1-\epsilon)/V_p \tag{38}$$

and the surface area per unit volume is

$$a_v = A_p\,(N/V) = (A_p/V_p)(1-\epsilon) \tag{39}$$

Knowing the geometry of the particles and the void fraction in a bed allows us to determine a_v. Measurements of $\dot{Q}$ and $\Delta T_{\ln}$ then allow one to compute $h_{\ln}$ from Equation (35).

In order to correlate heat transfer data for packed beds we must decide upon a characteristic length and a characteristic velocity. The quantities should be chosen with the idea that there should be a strong correlation between the heat transfer rate and the characteristic length and velocity. A little thought should lead one to the conclusion that the characteristic length should be a measure of either the *size of the packing* or the *size of the void spaces* through which the fluid flows. We shall see shortly that the hydraulic radius R_h is related both to the packing size and the void space, and is therefore an especially suitable choice for a characteristic length. The hydraulic radius is traditionally used to characterize turbulent flow in noncircular ducts and is defined by (*41*)

$$R_h = \left(\frac{\text{cross section available for flow}}{\text{wetted perimeter of the cross section}}\right) \tag{40}$$

For straight channels or ducts the hydraulic radius is easily computed; however, for a packed bed this definition must be extended as follows (3)

$$\begin{aligned} R_h &= \left(\frac{\text{cross section available for flow}}{\text{wetted perimeter of the cross section}}\right) \\ &= \left(\frac{\text{volume of the bed available for flow}}{\text{wetted surface within the bed}}\right) \\ &= \left(\frac{\text{void volume/total volume}}{\text{wetted surface/total volume}}\right) \\ &= \epsilon/a_v \end{aligned} \tag{41}$$

Note that in this definition of R_h the wetted surface of the walls of the bed are neglected relative to the wetted surface of the packing. We may now use our previously derived expression for a_v to express R_h as

$$R_h = \left(\frac{V_p}{A_p}\right)\frac{\epsilon}{1-\epsilon} \tag{42}$$

Rather than use R_h as the characteristic length we will use six times the hydraulic radius so that L^* is given by

$$L^* = 6\,R_h = \left(\frac{6V_p}{A_p}\right)\left(\frac{\epsilon}{1-\epsilon}\right) \tag{43}$$

We now define the particle diameter D_p as

$$D_p \equiv 6V_p/A_p \tag{44}$$

so that our expression for the characteristic length becomes

$$L^* = D_p\left(\frac{\epsilon}{1-\epsilon}\right) \tag{45}$$

The definition for D_p given by Equation (44) was chosen so that the particle diameter for a sphere is the actual diameter of the sphere.

In choosing a characteristic velocity, it seems logical that the average velocity of the fluid flowing in the void space $\langle v_z \rangle$ would be most suitable. This velocity is defined by

$$\langle v_z \rangle = \frac{1}{A_{\text{void}}}\int_{A_{\text{void}}} v_z\, dA \tag{46}$$

Here A_{void} is the void area contained within any cross section of the bed. If the bed is *uniform*, A_{void} and $\langle v_z \rangle$ are constant throughout the bed. The volumetric flow rate Q is given by

$$Q = \int_{A_{\text{void}}} v_z\, dA \tag{47}$$

and the void area is related to the cross sectional area of the bed A by the expression (*42*)

$$A_{\text{void}} = \epsilon\, A \tag{48}$$

We can now express our characteristic velocity as

$$u^* = \langle v_z \rangle = Q/\epsilon A \tag{49}$$

The volumetric flow rate divided by the cross sectional area is referred to as the *superficial velocity*

$$\text{superficial velocity} = Q/A \tag{50}$$

and is often used as a characteristic velocity for fixed bed catalytic chemical reactors. The superficial velocity is of course completely insensitive to variations in void fraction and is therefore judged to be a less suitable characteristic velocity.

At this point we have chosen our characteristic length and velocity,

$$L^* = D_p\left(\frac{\epsilon}{1-\epsilon}\right)$$

$$D_p = 6V_p/A_p$$

$$u^* = Q/\epsilon A$$

and we can now express the Reynolds number and Nusselt number as

$$N_{Re} = u^* L^*/\nu = \rho Q D_p/\mu A(1-\epsilon) = D_p G/\mu(1-\epsilon) \tag{51}$$

$$N_{Nu} = hL^*/k = \left(\frac{hD_p}{k}\right)\left(\frac{\epsilon}{1-\epsilon}\right) \tag{52}$$

Here G is the mass velocity equal to $\rho Q/A$. Our choice of characteristic length and velocity have led us to a Reynolds number and Nusselt number having the term $(1-\epsilon)$ in the denominator. We must therefore expect that as the void fraction becomes large our characteristic length and velocity will become unsuitable for $(1-\epsilon)^{-1}$ varies exceedingly rapidly as ϵ approaches unity.

We should remember that our dimensional analysis indicated that

$$N_{Nu} = F(N_{Re}, N_{Pr}, \mu_b/\mu_0, N_{BC}) \tag{53}$$

where N_{BC} represented all the dimensionless parameters appearing in the boundary conditions. Up to this point we avoided the problem of parameters appearing in the boundary conditions, for aside from a possible effect of wall roughness on heat transfer in a pipe, no parameters have arisen from the boundary conditions other than the effect of L/D contained in Equation (20). Now, however, we are confronted with very complex boundary conditions and we might well expect that other factors besides N_{Re}, N_{Pr} and μ_b/μ_0 would affect the Nusselt number.

All of the experimental data for heat transfer in packed beds are for air (*16, 17, 24, 39, 43*) with the exception of the results of Glaser and Thodos (*17*) who worked with nitrogen. The data are presented in Figure 6 and compare quite favorably with the equation

$$N_{Nu} = (0.5\, N_{Re}^{1/2} + 0.2\, N_{Re}^{2/3})\, N_{Pr}^{1/3} \tag{54}$$

The functional dependence on the Reynolds number clearly was motivated by the success of this form for fitting Nusselt numbers for single spheres and cylinders. There are several important points about this correlation which must be noted:

1. The Prandtl number dependence was chosen by the original investigators, but it remains unsubstantiated since there was negligible variation of the Prandtl number in the experimental studies. In the next section on staggered tube bundles there are results which indicate that the one-third power is reasonable.

2. The data in Figure 6 represent an enormous range of packings primarily because of the extensive study by Taecker and Hougen. They performed experiments for three sizes of Raschig Rings, one size Partition Ring, and two sizes of Berl Saddles. Their range of particle geometries is certainly extensive and yet the results can be correlated with a single equation *provided* one uses the appropriate Nusselt number and Reynolds number. This is shown more clearly in Figure 7 where all the data obtained by Taecker and Hougen are plotted along with all the data of Glaser and Thodos for spheres and cylinders.

3. The data for cubes obtained by Glaser and Thodos lie significantly below the other data. This is presumably due to the reduction of the effective surface area that can occur when two or more cubes become stacked.

4. The high void fraction data ($\epsilon = 0.78$) of McConnachie and Thodos are *significantly* higher than the other

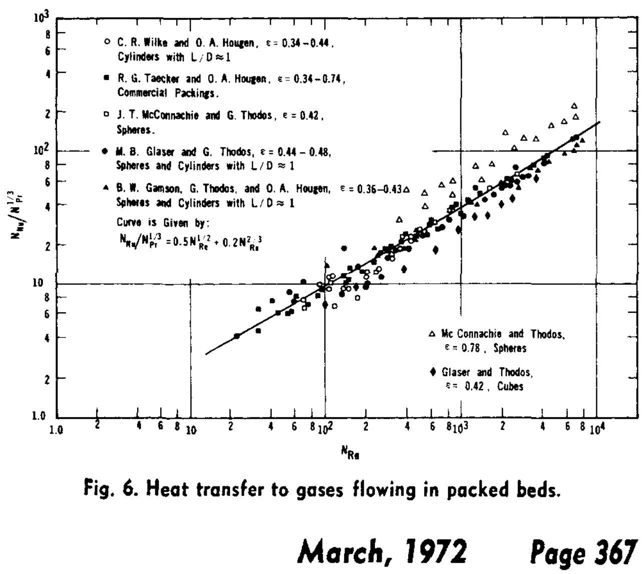

Fig. 6. Heat transfer to gases flowing in packed beds.

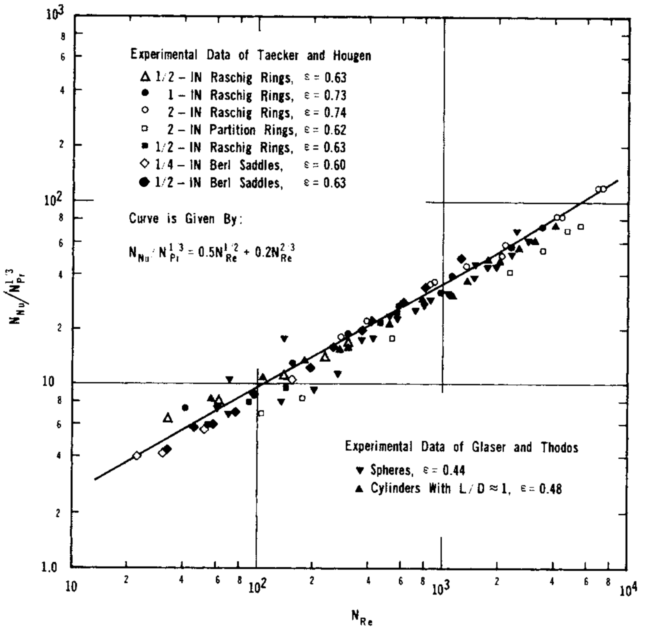

Fig. 7. Heat transfer to gases flowing in packed beds.

data. This would seem to indicate that the correlation may not be valid for large values of the void fraction; however, the data of Taecker and Hougen contain void fractions which are nearly as large as the value of 0.78. Another explanation is that all the data shown in Figure 6 are for *randomly* packed beds with the exception of the data of McConnachie and Thodos who constructed body-centered cubic arrangements of spheres for their packed beds. With this type of regular geometry it seems likely that parameters describing the geometry of the bed would be needed to complete the correlation. Data for tube bundles seem to indicate the geometrical effects become more pronounced as the arrangement of the heat transfer surface becomes more regular, that is, having less of a random nature.

If we discard the high void fraction data of McConnachie and Thodos and the data of Glaser and Thodos for cubes we can conclude that Equation (54) represents a satisfactory correlation for heat transfer in randomly packed beds of spheres, cylinders, Raschig rings, partition rings, and Berl saddles. For these cases the correlation can be considered accurate to better than ± 25%.

FLOW IN STAGGERED TUBE BUNDLES

Because of the success obtained in correlating heat transfer data for a wide variety of packed beds, it seemed reasonable to apply the correlation to heat transfer in tube bundles. In this section heat transfer data for staggered tube bundles will be considered. The geometrical configuration is illustrated in Figure 8. The geometry of the tube bundle can be specified in terms of D, s_t, and s_l provided the length of the tubes is much larger than the diameter, and provided the tube bundle contains at least ten rows of tubes. Under these circumstances entrance and edge effects are negligible and the functional dependence of the Nusselt number can be expressed as

$$N_{Nu} = F(N_{Re}, N_{Pr}, \mu_b/\mu_0, S_l, S_t) \quad (55)$$

Here we have replaced N_{BC} in Equation (53) with the dimensionless parameters S_l and S_t which are defined by

$$S_l = s_l/D \quad (56)$$

$$S_t = s_t/D \quad (57)$$

Drawing upon our experience with packed beds we propose *essentially the same correlation* for staggered tube bundles, that is

$$N_{Nu} = (0.5\, N_{Re}^{1/2} + 0.2\, N_{Re}^{2/3})\, N_{Pr}^{1/3}\, (\mu_b/\mu_0)^{0.14} \quad (58)$$

This correlation is compared with a wide range of experimental data (*1, 2, 20, 30*) in Figure 9. There are a number of important points to be noted regarding Figure 9:

1. Provided $N_{Re} \geqq 10^2$ and $\epsilon \leqq 0.65$ the same correlation, corrected for the effect of variable viscosity, that we used to predict heat transfer rates in packed beds can be used for staggered tube bundles.
2. The data in Figure 9 represent Prandtl numbers ranging from approximately 0.7 to 30 with the exception of the low Reynolds number data of Bergelin, Colburn, and Hull. Prandtl numbers for that data are on the order of 290 to 760. Because of the limited Prandtl number variation in the range of Reynolds numbers from 10^2 to 10^4 one cannot consider the one-third power on the Prandtl number to be experimentally confirmed. In view of the fact that the Prandtl number exponent ranged from 0.4 to 0.43 for turbulent flow in pipes, past flat plates, spheres and cylinders, we must continue to speculate that the $N_{Pr}^{1/3}$

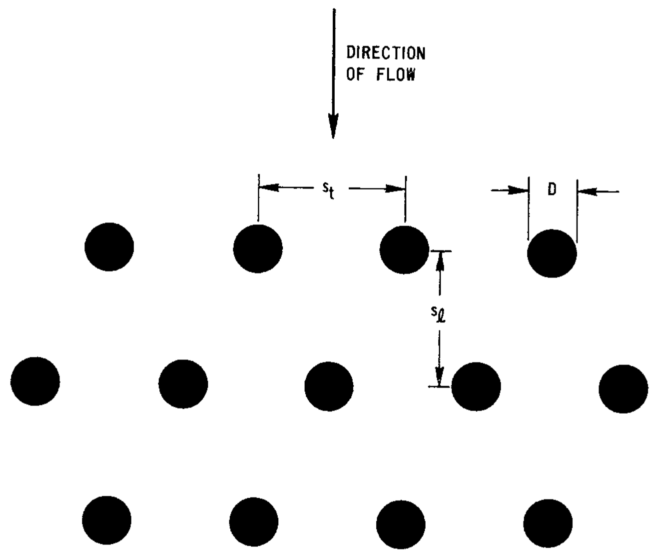

Fig. 8. Geometry for a staggered tube bundle.

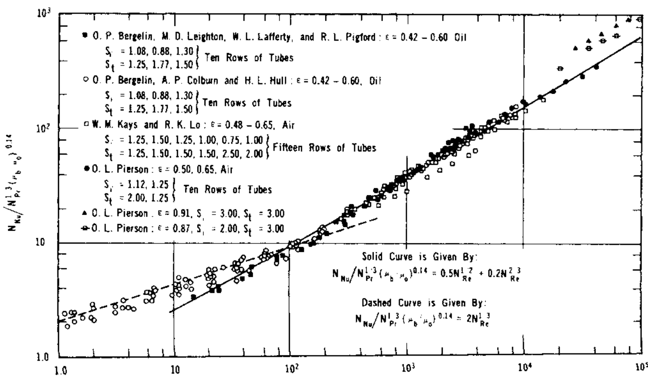

Fig. 9. Heat transfer to fluids flowing past staggered tube banks.

dependence is something less than the best functional dependence, but that it is satisfactory provided $N_{Pr} \leqq 30$.

3. For Reynolds numbers less than 10^2 the high Prandtl number data of Bergelin, Colburn, and Hull begins to deviate from the correlation expressed by Equation (58). It seems possible that this is caused by the interaction of the boundary layers with the neighboring tubes. We can estimate the thickness of the hydrodynamic boundary layer as

$$\delta \approx \sqrt{\nu x / u^*}$$

where x is the distance from the stagnation point at the front of the tube. One-quarter of the way around the tube we could estimate the boundary layer thickness as

$$\delta \approx \sqrt{\nu(\pi D/4)/u^*}$$
$$\approx D/N_{Re}{}^{1/2}$$

The boundary layers from adjacent tubes in the same row would interact when

$$\delta = \frac{D}{2}(S_t - 1), \quad \text{for interaction}$$

In terms of the Reynolds number, this means that interaction occurs when

$$N_{Re} \leqq \sqrt{2/(S_t - 1)} \approx 2$$

This crude order of magnitude estimate indicates that for low Reynolds numbers we can expect deviations from the Reynolds number dependence given by Equation (58), and the low Reynolds number data have been fit with the expression

$$N_{Nu} = 2\, N_{Re}{}^{1/3}\, N_{Pr}{}^{1/3}\, (\mu_b/\mu_0)^{0.14} \qquad (59)$$

This Reynolds number dependence was chosen on the basis of the Sieder-Tate correlation for heat transfer to laminar flow in a tube.

4. The data of Pierson for $\epsilon = 0.87$ and $\epsilon = 0.91$ clearly lie above the correlation. Although it is not obvious in Figure 9 these results indicate that the measured Nusselt numbers are about *twice* the value predicted by Equation (58), thus the correlation *does not* hold for large values of the void fraction. We should also note that the data of Pierson for $\epsilon = 0.50$ and $\epsilon = 0.65$ are in excellent agreement with the correlation. The failure of the correlation at high void fractions is in agreement with the packed bed data where the results of McConnachie and Thodos for $\epsilon = 0.78$ were higher than the value predicted by the correlation.

5. If one examines the work of an individual group of investigators one will generally find a correlation for each tube bundle configuration. This dependence on geometry is not completely removed by the proper choice of characteristic length and velocity; however, the variation of N_{Nu} detected by the same investigator for different geometries is comparable to the variation detected by different investigators for the same geometry, thus it would appear to be satisfactory at this time to use a single correlation for all the staggered tube bundle geometries provided $\epsilon \leqq 0.65$.

FLOW IN IN-LINE TUBE BUNDLES

The geometrical configuration for in-line tube bundles is illustrated in Figure 10, and once again our dimensional analysis would indicate that

$$N_{Nu} = F(N_{Re}, N_{Pr}, \mu_b/\mu_0, S_l, S_t)$$

The data for several investigators (*1, 12, 13*) are plotted in Figure 11 and compared with the correlation used successfully for staggered tube bundles. Clearly the correlation fails and the effect of S_l and S_t must be included in any correlation for heat transfer in in-line tube bundles.

CONCLUSIONS

Recent and not so recent forced convection heat transfer data have been collected and used to develop some minor variations on the traditional correlations. The parallel heat transfer process suggested by Richardson for bluff bodies appears to provide a satisfactory approach to correlating data for spheres, cylinders, packed beds and tube bundles. A proper choice of the characteristic length and velocity for packed beds and tube bundles has led to a single correlation which satisfactorily predicts heat transfer rates in randomly packed beds and staggered tube bundles.

ACKNOWLEDGMENT

In order to assemble the data presented in this paper, many investigators were asked to diligently search their files for the required tabulated data. They are too many to list here; they have my thanks.

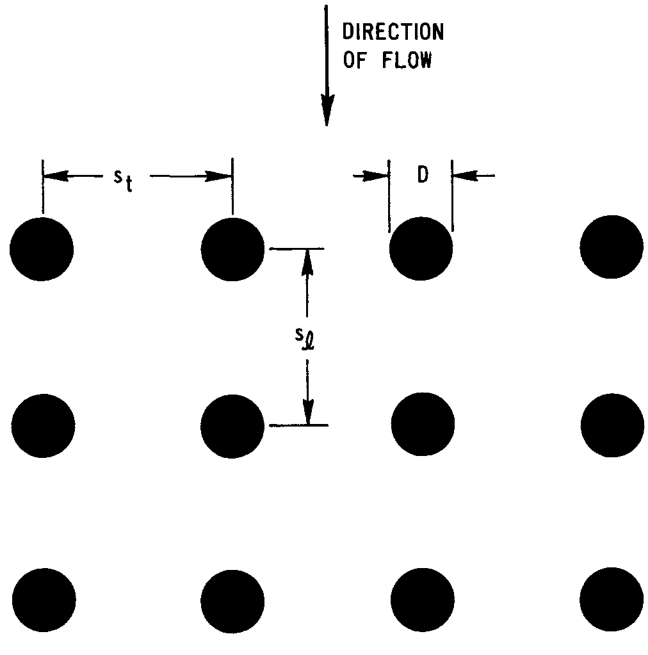

Fig. 10. Geometry for an in-line tube bundle.

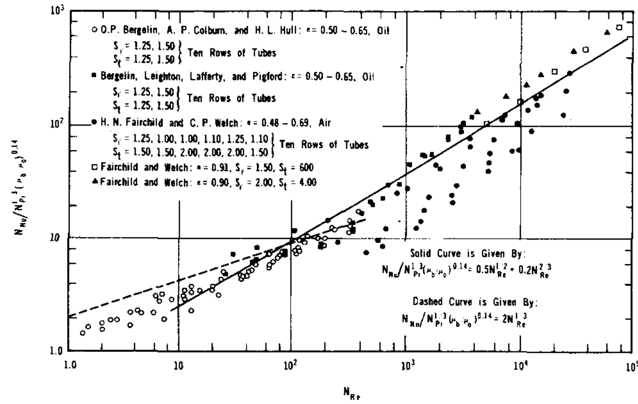

Fig. 11. Heat transfer to fluids flowing past in-line tube banks.

NOTATION

a_v = surface area per unit volume, sq.cm./cu.cm.
A_p = surface area of a particle or tube, sq.cm.
A = cross sectional area, sq.cm.
A^* = characteristic area, sq.cm.
A_{void} = void area, sq.cm.
c_p = constant pressure heat capacity, cal./g.-°C.
D = diameter, cm.
D_p = $6\ V_p/A_p$, particle diameter
G = mass velocity, g. cm./sec.
g = gravity vector, sq.cm./sec.
h = film heat transfer coefficient, cal./(sq.cm.)(sec.)(°C.)
h_{ln} = log mean film heat transfer coefficient, cal./(sq. cm.)(sec.)(°C.)
j = $(h/c_p\ G)N_{Pr}^{2/3}$, dimensionless parameter
k = thermal conductivity, cal./(cm.)(sec.)(°C.)
L = length, cm.
L^* = characteristic length, cm.
$\mathbf{n}$ = unit outwardly directed normal vector
N = number of particles
N_{Re} = u^*L^*/ν, Reynolds number
$N_{Re,L}$ = $u_x L/\nu$, length Reynolds number
$N_{Re,x}$ = $u_x x/\nu$, length Reynolds number
N_{Pr} = $c_p\mu/k$, Prandtl number
N_{Nu} = hL^*/k, Nusselt number
N_{BC} = dimensionless parameters appearing in the boundary conditions
p = fluid pressure, dynes/sq.cm.
P = $[(p - p^*)/\rho u^{*2}] + \phi/u^{*2}$, dimensionless pressure
$\dot{Q}$ = overall heat transfer rate, cal./sec.
Q = volumetric flow rate, cu.cm./sec.
R_h = hydraulic radius, cm.
s_t = transverse pitch, cm.
s_l = longitudinal pitch, cm.
S_t = s_t/D, dimensionless transverse pitch
S_l = s_l/D, dimensionless longitudinal pitch
T = temperature, °C.
T^* = characteristic temperature, °C.
T_∞ = temperature of the free stream flow past a bluff body, °C.
T_b = bulk or "cup mixing" temperature, °C.
T_0 = wall or surface temperature, °C.
T_f = $(T_b + T_0)/2$, film temperature, °C.
t = time, sec.
u^* = characteristic velocity, cm./sec.
$\mathbf{U}$ = $\mathbf{v}/u^*$, dimensionless velocity vector
$\mathbf{v}$ = fluid velocity vector, cm./sec.
v_z = z-component of the fluid velocity vector, cm./sec.
$\langle v_z \rangle$ = average value of v_z, cm./sec.
V = volume of a tube bundle or packed bed, cu.cm.
V_{void} = void volume of a tube bundle or packed bed, cu. cm.
V_p = volume of a packing particle or tube, cu.cm.
w = width of a flat plate, cm.
X, Y, Z = dimensionless rectangular Cartesian coordinates

Greek Letters

ΔT^* = characteristic temperature difference, °C.
ΔT_{ln} = log-mean temperature difference, °C.
δ = hydrodynamic boundary layer thickness, cm.
ϵ = V_{void}/V, void fraction
θ = tu^*/L^*, dimensionless time
Θ = $(T - T^*)/(T_0 - T^*)$, dimensionless temperature
Λ = $(\partial\mu/\partial\Theta)^*/\mu^*$, dimensionless viscosity parameter
μ = fluid viscosity, (dyne)(sec.)/sq.cm.
ρ = fluid density, g./cu.cm.
$\boldsymbol{\tau}$ = viscous stress tensor, dyne/sq.cm.
ϕ = gravitational potential energy function, sq.cm./sec.^{2}
Ψ = $(T_{b2} - T_{b1})/\Delta T_{ln}$, measured temperature function

Subscripts

0 = evaluated at the wall or surface
b = evaluated at the bulk temperature
∞ = evaluated at the free stream temperature
f = evaluated at the film temperature

Superscripts

$*$ = characteristic value

LITERATURE CITED

1. Bergelin, P. O., A. P. Colburn, and H. L. Hull, No. 2, Univ. Delaware Eng. Expt. Station (June, 1950).
2. Bergelin, O. P., M. D. Leighton, W. L. Lafferty, and R. L. Pigford, Bull. No. 4, Univ. Delaware Eng. Expt. Station, (April, 1958).
3. Bird, R. B., W. E. Stewart, and E. N. Lightfoot, "Transport Phenomena," Wiley, New York (1960).
4. Christiansen, E. B., and S. E. Craig, *AIChE J.*, **8**, 154 (1962).
5. Christiansen, E. B., G. E. Jensen, and Fan-Sheng Tao, *ibid.*, **12**, 1196 (1966).
6. Churchill, S. W., and J. C. Brier, *Chem. Eng. Progr. Symp. Ser. No.* **51**, 57 (1955).
7. Colburn, A. P., and C. A. Coghlan, *Trans. ASME*, **63**, 561 (1941).
8. Colburn, A. P., *Trans. Am. Inst. Chem. Engrs.*, **29**, 174 (1933).
9. Davis, A. H., *Phil. Mag.*, **47**, 1057 (1924).
10. Deissler, R. G., and C. S. Eran, NACA Tech. Note 2629 (1952).
11. Drew, T. B., *Ind. Eng. Chem.*, **24**, 152 (1932).
12. Edwards, A., and B. N. Furber, *Proc. Inst. Mech. Engrs.* (*London*) **170**, 941 (1956).
13. Fairchild, H. N., and C. P. Welch, Paper No. 61-WA-250, presented at ASME Ann. Mtg (1961).
14. Fand, R. M., *Intern. J. Heat Mass Transfer*, **8**, 995 (1965).
15. Friend, W. L., and A. B. Metzner, *AIChE J.*, **4**, 393 (1958).
16. Gamson, B. W., George Thodos, and O. A. Hougen, "Heat, Mass, and Momentum Transfer in the Flow of Gases Through Granular Solids," *Trans. Am. Inst. Chem. Engrs.*, **39**, 1 (1943).
17. Glaser, M. B. and George Thodos, *AIChE J.*, **4**, 63 (1958).
18. Graetz, L., *Ann. Physik*, **25**, 337 (1885).
19. Hilpert, Von R., *Forsch. Gebiete Ingenieurw.*, **4**, 215 (1933).
20. Kays, W. M., A. L. London, and R. K. Lo, Trans ASME, **76**, 387 (1954).
21. Kramers, H., *Physica*, **12**, 61 (1946).
22. Lawrence, A. E., and T. K. Sherwood, *Ind. Eng. Chem.*, **23**, 301 (1931).
23. McAdams, W. H., "Heat Transmission," 3rd edn, McGraw-Hill, New York (1954).
24. McConnachie, J. T. L., and George Thodos, *AIChE J.*, **9**, 60 (1963).
25. Metzner, A. B., in Advances in Heat Transfer, J. P. Hartnet and T. F. Irvine, Jr., (eds. Academic Press, New York (1965).
26. Morris, F. H., and W. G. Whitman, *Ind. Eng. Chem.*, **20**, 234 (1928).
27. Notter, R. H., and C. A. Sleicher, unpublished manuscript (April, 1971).
28. Parmelee, G. V., and R. G. Huebscher, *Heating, Piping, and Air Conditioning*, **19**, 8, 115, (1947).
29. Perkins, H. C., and G. Leppert, *J. Heat Transfer, Trans. ASME, Series C*, **84**, 257 (1962).
30. Pierson, O. L., Trans. ASME, **59**, 563 (1931).
31. Piret, E. L., W. James, and M. Stacy, *Ind. Eng. Chem.*, **39**, 1098 (1947).
32. Reynolds, W. C., W. M. Kays, and J. S. Kline, Dept. of Mech. Engr., Stanford Univ., NACA rept. for contract NAW-6494 (1957).

33. Richardson, P. D., WADD TN-59-1 (1968).
34. Schlichting, H., "Boundary Layer Theory," 6th ed., McGraw-Hill, New York (1960).
35. Schneider, P. J., *Trans. ASME*, 79, 765 (1957).
36. Schubauer, G. B., and H. K. Skramstad, *NACA Rept. 909*, 1949.
37. Sieder, E. N., and G. E. Tate, *Ind. Eng. Chem.*, **28**, 1429 (1936).
38. Sherwood, T. K., and J. M. Petrie, *Ind. Eng. Chem.*, **24**, 736 (1932).
39. Taecker, R. G., and O. A. Hougen, *Chem. Eng. Progr.*, **45**, 188 (1949).
40. Vliet, G. C., and G. Leppert, *J. Heat Transfer, Trans. ASME, Series C*, **83**, 163 (1961).
41. Whitaker, S., *Introduction to Fluid Mechanics*, Prentice-Hall, Englewood Cliffs, N. J. (1968).
42. ———, *Ind. Eng. Chem.*, **61**, 14 (1969).
43. Wilke, C. R., and O. A. Hougen, *Trans. Am. Inst. Chem. Engrs.*, **41**, 445 (1945).
44. Yuge, T., *J. Heat Transfer, Trans. ASME, Series C*, **82**, 214 (1960).
45. Zhukauskas, A. A., and A. B. Ambrazyavichyus, *Intern. J. Heat Mass Transfer*, **3**, 305 (1961).
46. King, L. V., *Phil. Trans. Roy. Soc. (Lond.)*, **214**, 373 (1914).
47. Kelsey, S. J., and E. B. Christiansen, paper presented at the AIChE Nat. Mtg., Cincinnati (May, 1971).
48. Collis, D. C., and M. J. Williams, *J. Fluid Mech.*, **6**, 357 (1959).

APPENDIX: J-FACTOR VERSUS NUSSELT NUMBER

In 1933 A. P. Colburn (*8*) suggested a new method of plotting heat transfer data so that some correspondence between energy and momentum transfer was illustrated. This method consisted of plotting the now famous *j*-factor versus the Reynolds so that an analogy between the friction factor and the *j*-factor existed.

Following the development presented by Colburn we define the Nusselt number for turbulent flow in a pipe as

$$N_{Nu} = hD/k \tag{A1}$$

where the film heat transfer coefficient is related to the overall heat transfer rate by the definition

$$\dot{Q} = h\Delta T^{*}\ A^{*} \tag{A2}$$

Here ΔT^{*} is some characteristic temperature difference and A^{*} is some characteristic area. These are traditionally taken to be

$$\Delta T^{*} = \Delta T_{\ln} = \frac{(T_{b2} - T_{02}) - (T_{b1} - T_{01})}{\ln\left(\dfrac{T_{b2} - T_{02}}{T_{b1} - T_{01}}\right)} \tag{A3}$$

$$A^{*} = \pi\ D\ L \tag{A4}$$

If the axial transport of energy can be entirely attributed to the time averaged convective transport, that is, axial conduction and dispersion are negligible, the macroscopic thermal energy balance for an incompressible flow yields

$$Q = \rho\langle v_z\rangle \left(\frac{\pi D^2}{4}\right) c_p\,(T_{b2} - T_{b1}) \tag{A5}$$

Making use of Equations (A2) through (A5) allows us to express the Nusselt number as

$$\begin{aligned} N_{Nu} &= \frac{\rho\langle v_z\rangle(\pi D^2/4)\ c_p\ D\ (T_{b2} - T_{b1})}{\Delta T_{\ln}\ (\pi DL)k} \\ &= N_{Re}\ N_{Pr}\,(D/4L)\ [(T_{b2} - T_{b1})/\Delta T_{\ln}] \end{aligned} \tag{A6}$$

At this point Colburn notes that it is the functional dependence of $(T_{b2} - T_{b1})/\Delta T_{\ln}$ that the experimentalist seeks to determine and that one should plot the measured temperature function

$$\frac{T_{b2} - T_{b1}}{\Delta T_{\ln}} = \Psi = \frac{N_{Nu}}{N_{Re}N_{Pr}(D/4L)} \tag{A7}$$

against the Reynolds number. This argument led to the use of the *j*-factor

$$j = \left(\frac{T_{b2} - T_{b1}}{\Delta T_{\ln}}\right)\left(\frac{4L}{D}\right) N_{Pr}{}^{2/3} \tag{A8}$$

as a correlating variable. If we examine Equation (A6) we see the motivation for Colburn's warning against "plotting a funcotin against itself"; however, a little analysis will show that plotting the Nusselt number against the Reynolds number has no disadvantages.

We begin by writing Equation (A6) as

$$N_{Nu} = N_{Re}N_{Pr}\,(D/4L)\ \Psi \tag{A9}$$

where Ψ is essentially equivalent to the *j*-factor. The true functional relation between the Nusselt number and the Reynolds number will be denoted by

$$\overline{N}_{Nu} = G(N_{Re}) \tag{A10}$$

and from Equation (A9) we obtain the true functional relation between Ψ and N_{Re}.

$$\overline{\Psi} = G(N_{Re})/N_{Re}N_{Pr}\,(D/4L) \tag{A11}$$

Let the error in the measured value of Ψ be $\delta\Psi$ so that

$$\Psi = \overline{\Psi} + \delta\Psi \tag{A12}$$

The error in the measured Nusselt number is therefore*

$$\delta N_{Nu} = N_{Re}\,N_{Pr}\,(D/4L)\ \delta\Psi \tag{A13}$$

and the fractional error in the Nusselt number is

$$\frac{\delta N_{Nu}}{\overline{N}_{Nu}} = \frac{N_{Re}\,N_{Pr}\,(D/4L)\ \delta\Psi}{G(N_{Re})} \tag{A14}$$

Making use of Equation (A11) we can put Equation (A14) in the form

$$\frac{\delta N_{Nu}}{\overline{N}_{Nu}} = \frac{\delta\Psi}{\overline{\Psi}} \tag{A15}$$

indicating that the fractional error in N_{Nu} is the same as the fractional error in Ψ. Thus there would appear to be no clear cut advantage in plotting *j*-factors instead of Nusselt numbers. This is illustrated in Figure A1 where we have plotted $(N_{Nu} - 2)/N_{Re}\,N_{Pr}{}^{0.4}\,(\mu_b/\mu_0)^{1/4}$ against N_{Re}. Clearly there is no preference for this form of the correlation over that given in Figure 4.

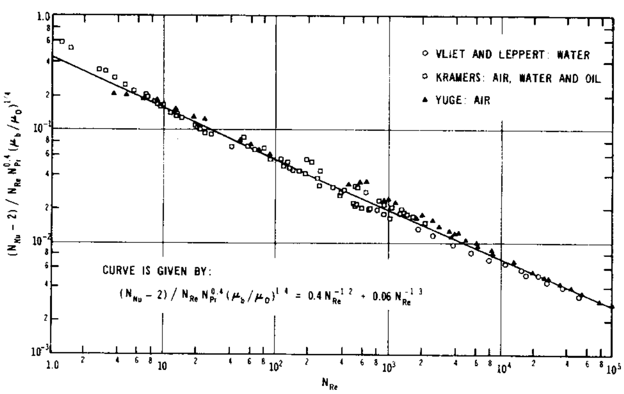

Fig. A1. Heat transfer to fluids flowing past a single sphere.

* Here we have assumed negligible error in N_{Re} and N_{Pr} relative to the error in Ψ.

Manuscript received June 15, 1971; revision received September 15, 1971; paper accepted September 16, 1971.